

# Negative-Unlabeled Tensor Factorization for Location Category Inference from Inaccurate Mobility Data

Jinfeng Yi<sup>1</sup>, Qi Lei<sup>\*2</sup>, Wesley Gifford<sup>1</sup>, and Ji Liu<sup>3</sup>

<sup>1</sup>IBM Thomas J. Watson Research Center

<sup>2</sup>University of Texas at Austin

<sup>3</sup>Computer Science Department, University of Rochester

## Abstract

Identifying significant location categories visited by mobile phone users is the key to a variety of applications. This is an extremely challenging task due to the possible deviation between the estimated location coordinate and the actual location, which could be on the order of kilometers. Using the collected location coordinate as the center and its associated location error as the radius, we can draw a location uncertainty circle that may cover multiple location categories, especially in densely populated areas. To estimate the actual location category more precisely, we propose a novel tensor factorization framework, through several key observations including the intrinsic correlations between users, to infer the most likely location categories within the location uncertainty circle. In addition, the proposed algorithm can also predict where users are even when there is no location update. In order to efficiently solve the proposed framework, we propose a parameter-free and scalable optimization algorithm by effectively exploring the sparse and low-rank structure of the tensor. Our empirical studies show that the proposed algorithm is both efficient and effective: it can solve problems with millions of users and billions of location updates, and also provides superior prediction accuracies on real-world location updates and check-in data sets.

## 1 Introduction

Understanding mobile phone users' spatio-temporal activities is a central theme in a variety of applications, including personalized advertising [3], traffic monitoring [19], security management [33], and assistance of the elderly and disabled [4]. To this end, a key step is to identify the significant location categories visited by each mobile phone user from his / her mobile location updates, such as restaurants, gyms, and shopping malls. Unfortunately, this is an extremely challenging task since mobile location updates are often highly inaccurate. Inaccuracies arise for a number of reasons, for example,

- **signal conditions and qualities:** In GPS-based systems signal conditions, such as dense foliage or urban canyons, can impact the ability to communicate with the required number of satellites or introduce delay in signal propagation – ultimately leading to decreased accuracy.

---

<sup>\*</sup>Part of the work was done during Qi Lei's internship at IBM Thomas J. Watson Research Center.

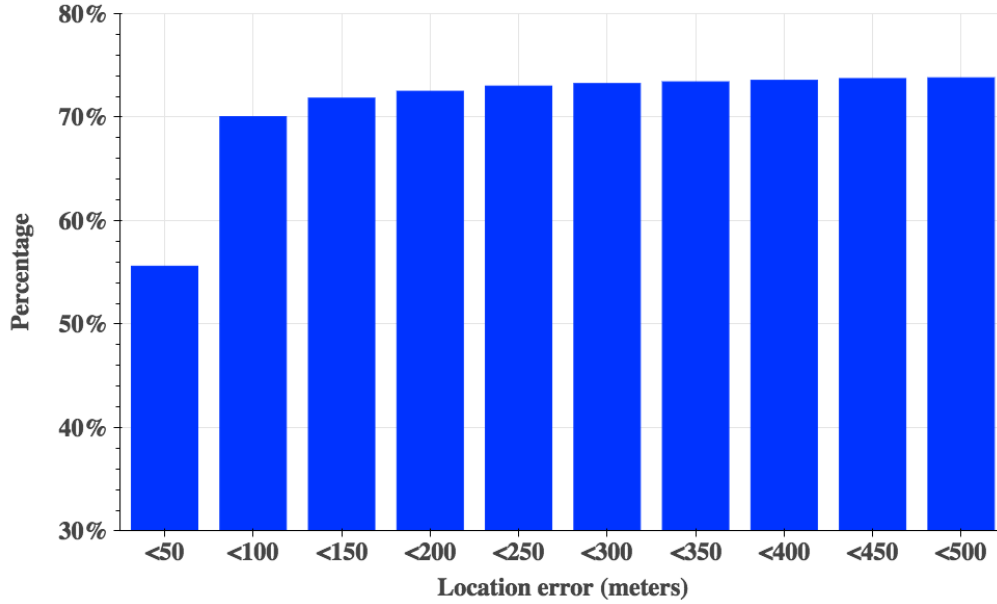


Figure 1: Histogram of mobile phone location errors for a large anonymized sample of mobile location data.

- **bias of location estimation techniques:** For triangulation-based methods, the density of WiFi or cellular networks can significantly affect accuracy. The fact that the density of such networks varies significantly across locations means different levels of accuracy will be observed.
- **device limitation:** Many mobile applications may deliberately request less frequent or less accurate location information in order to conserve battery power for applications where high accuracy is not explicitly required.

Using a sample of mobile location data collected as part of an IBM partnership with a leading location-based services company, we investigated the distribution of location errors. The error distribution for one month of data from a major U.S. city is depicted in Figure 1. The data show that only 56% of updates have errors within 50 meters, while 26% of the updates have errors greater than 500 meters. Using the estimated location coordinate as the center and its associated error as the radius, we can draw a circle where the mobile phone user may be located. We refer to such a circle as *location uncertainty circle*, which may cover multiple location categories, especially in densely populated areas like cities. Figure 2 shows a location uncertainty circle drawn based on a simulated location update and a 100 meter location error in New York City. Although this circle is not very large, it still covers 7 location categories, including library, restaurant, school, shop, gallery, bank, and consulate, all of which might be the true venue visited by this user. To decide a unique location category, a naive idea is to use 1-nearest neighbor (1-NN) approach, i.e., simply choose the venue that is closest to the estimated location coordinate. However, this approach is problematic since there may exist multiple nearby venues with almost identical distances to the estimated location coordinate. Figure 2 gives one such example. The estimated location coordinate is almost equally close to the boundaries of four venues, including a Chase bank, a pizza restaurant, a clothing shop, and the New York Society Library. Therefore, it is almost impossible to identify the true venue

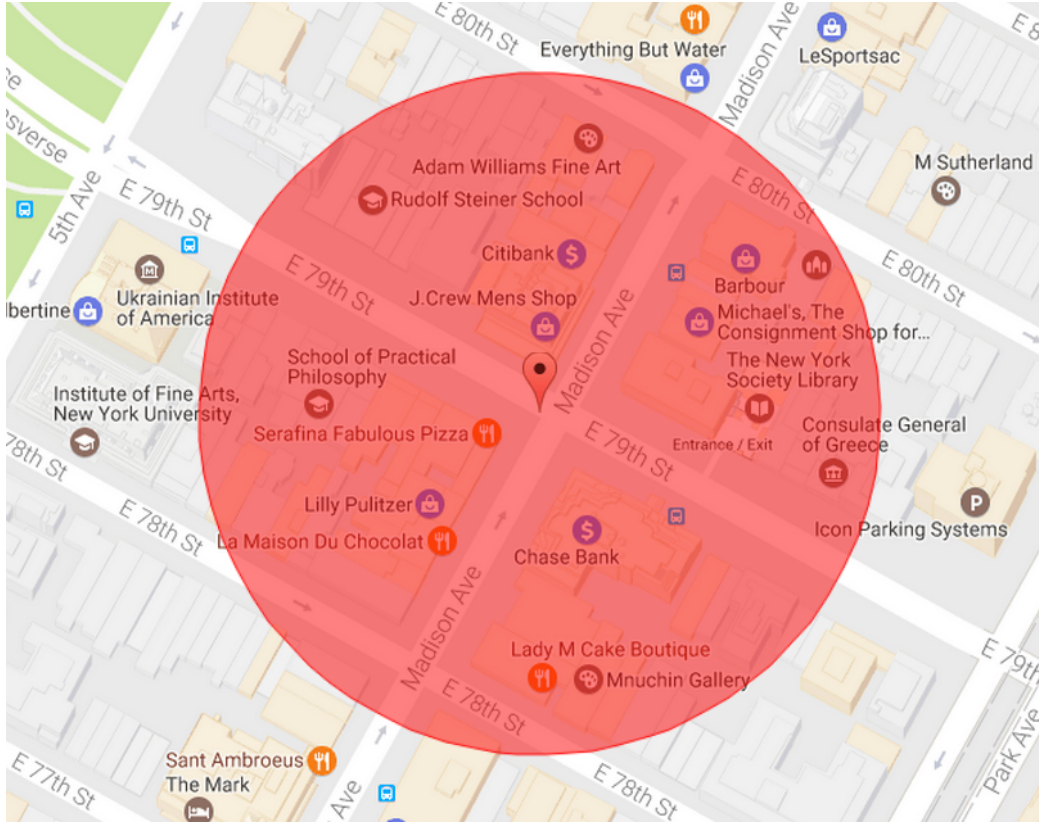


Figure 2: A simulated location uncertainty circle with a 100-meter radius in New York City. It covers location categories *library*, *restaurant*, *school*, *shop*, *gallery*, *bank*, and *consulate*.

using the 1-NN approach. In addition, since many location updates have very large location errors, and the estimated location coordinate could be highly biased, there is no guarantee that the true venue visited by the mobile phone user is close to the estimated location coordinate.

In this paper, we study the problem of inferring mobile phone users' true location categories based on noisy location updates. This problem is challenging since many location errors are fairly large, and hence users' underlying true locations may be far away from the estimated coordinates. In addition, since mobile users are anonymous and we have no access to their personal information, no side information other than the noisy mobility location data itself is used in our modeling, which further increases the difficulty.

In this paper, we develop a novel framework for location category inference to address these challenges, based on some key observations and the intrinsic correlations among users. Given a collection of location updates that involve a total of  $N$  mobile phone users,  $T$  time slots, and  $C$  location categories, our objective is to learn a non-negative three-way tensor  $\mathcal{X} \in \mathbb{R}_+^{N \times T \times C}$  where  $\mathcal{X}_{ijk}$  indicates the probability that user  $i$  visited the location category  $k$  during the time slot  $j$ . To this end, we first observe that for each location update, there is one and only one true location category since a user can only visit one place at a time. In addition, since the user's true location must be within the location uncertainty circle, the location categories not covered by this circle cannot be visited. Therefore, the probabilities of visiting these location categories is zero, while the

probabilities of location categories covered by the location uncertainty circle sum up to one. Indeed, we can treat this problem as a two-class learning problem where the positive class contains only one example (i.e., the true location category) while all the other examples belong to the negative class (i.e., false location categories). Under this scenario, all the labeled examples are sampled from the negative class and the unlabeled examples come from both negative and positive classes. We refer to such a problem as a *negative-unlabeled (NU) learning* problem, a counterpart to the positive-unlabeled (PU) learning problem [8, 17, 12] or the problem of learning from implicit feedback in the recommendation literature [13, 22, 2]. The key feature to these problems is that the labeled examples are only drawn from the positive class, and the unlabeled examples are a mixture of positive and negative class samples.

The observations specified above are insufficient to recover the probabilities of all the location categories since we can assign the non-zero probabilities with any non-negative values that sum to one. To address this issue, we develop a collaborative approach that exploit all users' location updates to collaboratively locate each other. This is due to the reason that people with the same lifestyle tend to behave similarly. For instance, parents of kindergarteners may drop-off and pick-up their children at roughly the same local time, even if their children are not enrolled in a same kindergarten. Likewise, people with routine work-home schedules tend to go to work from home and go back home after work at similar time, which are the main reasons of morning and evening traffic peaks. In addition to user-user similarity, time-time similarity is another factor we can take advantage of since users' routines are usually consistent from day to day, or from week to week. This observation suggests that the underlying tensor  $\mathcal{X}$  should be close to low-rank, which is also verified by a widely held assumption that people's behaviors are dictated by a small number of latent factors [25, 32].

Given the above observations, we first formulate our learning problem as a low-rank tensor factorization problem under NU constraints. However, the high computational cost significantly limits its application to real-world location category inference problem that involves a large number of mobile phone users and location updates. To address this limitation, we first relax the problem to a matrix optimization problem by converting two three-way tensors to their mode-1 matricizations. We note that the problem after relaxation is still challenging to solve since it requires computation of a low-rank approximation of a large matrix, which is computationally expensive in general. More severely, the optimization problem involves  $N \times T \times C$  entries, thus a naive optimization algorithm will take at least  $O(N \times T \times C)$  time to optimize the problem. To overcome this limitation, we develop an efficient alternating minimization algorithm by effectively exploring the sparsity of the large matrix. Our experiments show that our algorithm is extremely efficient and can scale up to problems with millions of users. For instance, our synthetic study shows that the proposed algorithm is able to *perfectly* predict the underlying location categories for 3 million mobile phone users and close to a billion location updates in less than 1 hour.

Furthermore, we emphasize the key reasons why we specifically focus on the problem of inferring the true location category rather than the actual venue. Firstly, the number of venues is substantially larger than the number of categories. Since the number of users having venue-wise similar behavioral patterns is substantially lower than the number of users having category-wise similar behavioral patterns, it becomes very difficult to leverage collaborative techniques if individual venues are sought. More importantly, knowledge of the categories visited by users often provides enough useful information for many important tasks, such as profile estimation and personalized advertising.

Our main contributions in this paper are highlighted as follows:

- To the best of our knowledge, this is the first work that can infer users' location categories purely based on highly inaccurate mobility data. Specifically, we propose a novel learning framework that can not only infer location categories in a collaborative manner, but also handle the issues when large number of users' location updates are sparse and noisy.
- To the best of our knowledge, this is the first work that studies the tensor factorization problem under the negative-unlabeled (NU) constraints. One advantage of casting the location category inference problem as a tensor factorization problem is that by completing the tensor, we can even infer users' location categories when there is no location update data available.
- By effectively exploiting sparsity, we develop an extremely efficient algorithm that is able to infer location categories with a huge number of mobile phone users and location updates.

## 2 Related Work

To the best of our knowledge, this paper makes the first attempt to learn mobile phone users' location categories from highly inaccurate mobility location data. We review two existing works related to our work: stay point detection and location semantic meaning identification.

**Stay point detection** In a trajectory or sequence of location updates, stay points are defined as the important locations where people have stayed for a while [32]. [16] proposed the first stay point detection algorithm that checks if the distance and the time span between an anchor point and its successors in a trajectory are larger than two individual thresholds. If both answers are yes, a stay point is detected. The authors in [30, 31] further improved this algorithm by considering the density of location points. In [6], stay points were detected by modeling location-location and location-user relationships via a graph-based approach.

**Location semantic meaning identification** To go one step further, many location-aware applications also care about the semantic meanings of stay points. To address this problem, a typical idea is to first cluster the stay points to identify regions of interest, and then use a cluster ID to represent stay points belonging to this cluster. Popular clustering approaches in this area include time-based clustering, density-based clustering, and partitioning clustering, as summarized in [34]. In particular, the authors in [1] use a variant of  $k$ -means algorithm to cluster GPS data for detecting users' significant locations. Besides, a density-based clustering algorithm was applied in [29] to infer individual life patterns from GPS trajectory data. The authors in [26] estimate user similarities in terms of semantic location history using a hierarchical clustering-based approach. The work in [18] identifies home and work locations by first transforming user trajectory records into user-location signatures, and then applying  $k$ -Means clustering on these signatures.

**Key differences from our work** Although the problems discussed above share some similarities with our work, they differ from the focus of our paper in the following respects:

- They usually use accurate location data such as GPS signals to generate trajectories and ignore the location errors. On the contrary, the real-world mobile location update data considered in our study is highly inaccurate with unignorable location errors, making our problem much more difficult to solve.

- Given a location update in a trajectory, they aim to assign it to a cluster of similar location updates, under the assumption that similar location updates should belong to the same cluster. In comparison, our main focus is to infer the underlying true location category, under a more realistic scenario that even if two location updates appear to be similar, they may belong to different location categories due to unignorable location errors.
- Most studies mentioned above adopt non-collaborative approaches, where user’s profile data is used in isolation to determine his / her stay points. In contrast, the goal in this paper infers the user’s location categories altogether from a unified model that collaboratively locates each other. Comparing with non-collaborative approaches, our approach is more robust to inaccurate and sparse location updates data.

### 3 Methodology

In this section, we first briefly discuss how to clean up the raw mobility location update data and generate the candidate location categories. We then present our negative-unlabeled tensor factorization model, followed by a scalable optimization algorithm.

Throughout the paper, we use boldface Euler script letters, boldface capital letters, and boldface lower-case letters to denote tensors (e.g.,  $\mathcal{X}$ ), matrices (e.g.,  $\mathbf{X}$ ) and vectors (e.g.,  $\mathbf{x}$ ), respectively. The  $(i, j, k)$ -th entry of a third-order tensor  $\mathcal{X}$  and the  $(i, j)$ -th entry of a matrix  $\mathbf{X}$  is denoted by  $\mathcal{X}_{ijk}$  and  $\mathbf{X}_{ij}$ , respectively.  $|\Omega|$  returns the number of elements in the set of  $\Omega$ .  $[N]$  denotes the set  $\{1, 2, \dots, N\}$  for short, where  $N$  must be an integral number.

#### 3.1 Data Preprocessing and Location Candidate Generation

Given a collection of mobile location updates in the form  $\{\text{anonymous user id, UTC timestamp, estimated location coordinates, location error}\}$ , we first preprocess the raw data. The preprocessing encompasses three key steps: 1) filtering to retain only meaningful location updates, 2) association with location updates with category information, and 3) quantization of time into time slots. The specifics of how this is done is dependent on the data source used, and will be explained in more detail when the experiments are described in Section 4.

Once the preprocessed location update data, containing  $N$  users,  $T$  time slots, and  $C$  location categories, is available we construct the possible category set for each user at each time slot

$$\Omega_{ij} := \{k \in [C] \mid \text{category } k \text{ appears in} \\ \text{the location circle of user } i \text{ at time slot } j.\}$$

#### 3.2 A Negative-Unlabeled Tensor Factorization Model for Location Category Inference

Given a total of  $N$  users,  $T$  time slots,  $C$  location categories, and the possible location category set  $\Omega$ , our goal is to infer a location probability tensor  $\mathcal{X} \in \mathbb{R}_+^{N \times T \times C}$ . Each element  $\mathcal{X}_{ijk} \in [0, 1]$  denotes the probability of user  $i$  at time slot  $j$  visiting category  $k$ . Specifically, the larger the entry  $\mathcal{X}_{ijk}$ , the greater the chance that user  $i$  was visiting the location category  $j$  during the time slot  $k$ . To effectively infer the tensor  $\mathcal{X}$ , we need to restrict  $\mathcal{X}$  from several key observations.

The first observation is that if  $k \notin \Omega_{ij}$ ,  $\mathcal{X}_{ijk}$  must be 0. This is because a user cannot be visiting a location category if no venue in such category is within the error allowance of the location update. Our second observation is that among the location categories in  $\Omega_{ij}$ , there is one and only one true category since a user can only appear at one place at a time. In other words, we have  $\sum_{k \in \Omega_{ij}} \mathcal{X}_{ijk} = 1$ ,  $\forall i \in [N], j \in [T]$ . As an extreme case, the entry  $\mathcal{X}_{ijk}$  equals to 1 if there is only one location category located within the location uncertainty circle. Combining both observations 1 and 2, we face a scenario where (i) the positive (i.e., true location category) class contains only one example; (ii) all the labeled examples are sampled from the negative class (i.e., false location categories) and the unlabeled examples come from both negative and positive classes. We refer to such a scenario as *negative-unlabeled (NU)* setting. Therefore, together with the probability assumption of tensor  $\mathcal{X}$ , we can restrict it in the following region, in particular,  $\forall (i, j)$

$$\begin{cases} \mathcal{X}_{ijk} = 0, & \text{and } k \notin \Omega_{ij} \\ \sum_{k \in \Omega_{ij}} \mathcal{X}_{ijk} = 1, & \text{and } k \in \Omega_{ij} \\ \mathcal{X}_{ijk} \geq 0, & \forall k, \end{cases}$$

The two observations from *local* perspective specified above are insufficient to recover the tensor  $\mathcal{X}$  as we can fill its unobserved entries (i.e.,  $\mathcal{X}_{ijk}$ ,  $k \in \Omega_{ij}$ ) in with any non-negative values that add up to 1. To this end, we need to consider the inference of  $\mathcal{X}$  from a *global* perspective by integrating all users' trajectory data together to collaboratively locate each other, instead of learning a separate model for each user in isolation. The logic behind the collaborative approach is that people with the same lifestyle tend to behave similarly. For example, kindergarten parents may drop-off and pick-up their children at roughly the same local time, even if their children are not enrolled in the same kindergarten. Likewise, people with routine work-home style tend to go to work from home and go back home after work at similar time, which are the main reasons of morning and evening peaks. In addition to user-user similarity, time-time similarity is another factor we can take advantage of since users' trajectories are usually consistent from day to day or week to week. The observations above suggest that the underlying tensor  $\mathcal{X}$  should be close to low-rank. To see this, let's consider an ideal case where all the users belong to multiple lifestyle categories and the people with the same lifestyle behave the same. In this case, the rank of the location category tensor is upper bounded by the number of lifestyle categories, a typically small number. Indeed, the low-rank assumption can be verified by another view that people's daily trajectory paths are generally believed to be dictated by a small number of latent factors [25, 32].

Combining our observations together, we recover the tensor  $\mathcal{X}$  by solving the following negative-unlabeled tensor factorization (NUTF):

$$\min_{\mathcal{X}, \mathcal{Y} \in \mathbb{R}^{N \times T \times C}} \|\mathcal{X} - \mathcal{Y}\|_F^2 \quad (1)$$

$$\begin{aligned} \text{s.t.} \quad & \text{rank}(\mathcal{Y}) \leq r \\ & \begin{cases} \mathcal{X}_{ijk} = 0, \forall i, j, \text{ and } k \notin \Omega_{ij} \\ \sum_{k \in \Omega_{ij}} \mathcal{X}_{ijk} = 1, \forall i, j, \text{ and } k \in \Omega_{ij} \\ \mathcal{X}_{ijk} \geq 0, \forall i, j, k, \end{cases} \end{aligned} \quad (2)$$

where we require  $\mathcal{X}$  that satisfies the NU constraints (2) and also close to a low rank tensor  $\mathcal{Y}$  with rank no more than  $r$ . There are several choices for the definition of the rank of a tensor. We choose the one to make the optimization scalable, which will be clear soon.

---

**Algorithm 1** Projection of a vector onto the probability simplex [23]

---

- 1: **Input:** a vector  $\mathbf{v} \in \mathbb{R}^d$  to be projected
  - 2: Sort  $\mathbf{v}$  into  $\tilde{\mathbf{v}}$ :  $\tilde{v}_1 \geq \tilde{v}_2 \geq \dots \geq \tilde{v}_d$
  - 3: Find  $k = \max\{j \in [d] : \tilde{v}_j - \frac{1}{j}(\sum_{i=1}^k \tilde{v}_i - 1) > 0\}$
  - 4: Compute  $\theta = \frac{1}{k}(\sum_{i=1}^k \tilde{v}_i - 1)$
  - 5: **Return:**  $\mathbf{u} \in \mathbb{R}^d$  s.t.  $\mathbf{u}_i = \max(\mathbf{v}_i - \theta, 0)$ ,  $i \in [d]$
- 

### 3.3 A Parameter-free Scalable Optimization Algorithm

In order to efficiently solve the NUTF model (1), we adopt an alternating minimization scheme that iteratively fixes one of  $\mathcal{X}$  and  $\mathcal{Y}$  and minimizes with respect to the other. One nice property is that the proposed algorithm is *optimization parameter free*, that is, the user does not need to decide any optimization parameter such as step length or learning rate.

#### Update $\mathcal{X}$

In each iteration of the alternating minimization algorithm, we first update  $\mathcal{Y}$  with a fixed  $\mathcal{X}$ , and then update  $\mathcal{X}$  by fixing  $\mathcal{Y}$ . When  $\mathcal{Y}$  is fixed, our goal becomes learning a closest tensor that satisfies the NU constraints (2). To this end, we rewrite the objective function (1) by treating the entries lying within and outside of the  $\Omega$  set separately, i.e.,

$$\min_{\mathcal{X} \in \mathbb{R}^{N \times T \times C}} \sum_{i,j; k \notin \Omega_{ij}} (\mathcal{X}_{ijk} - \mathcal{Y}_{ijk})^2 + \sum_{i,j; k \in \Omega_{ij}} (\mathcal{X}_{ijk} - \mathcal{Y}_{ijk})^2 \quad (3)$$

$$\begin{cases} \mathcal{X}_{ijk} = 0, \forall i, j, \text{ and } k \notin \Omega_{ij} \\ \sum_{k \in \Omega_{ij}} \mathcal{X}_{ijk} = 1, \forall i, j, \text{ and } k \in \Omega_{ij} \\ \mathcal{X}_{ijk} \geq 0, \forall i, j, k \end{cases} \quad (4)$$

The optimization problem (3) consists of two independent and easily-computable subproblems. For the first subproblem that only involves the entries outside of the possible set  $\Omega$ , we simply set all of them as zeros to meet the NU constraints (2). The second subproblem only involves the entries lying within the possible set  $\Omega$  and is essentially a least square problem under a probability simplex constraint. Specifically, for each location update with user  $i$  and time slot  $j$ , we project a  $|\Omega_{ij}|$ -dimensional vector  $\mathcal{X}_{ij\Omega_{ij}}$  onto the probability simplex, which can be efficiently computed in  $O(|\Omega_{ij}| \log |\Omega_{ij}|)$  time, as described in Algorithm 1.

#### Update $\mathcal{Y}$

When  $\mathcal{X}$  is fixed, we update  $\mathcal{Y}$  by solving the following optimization problem:

$$\begin{aligned} \min_{\mathcal{Y} \in \mathbb{R}^{N \times T \times C}} \quad & \|\mathcal{X} - \mathcal{Y}\|_F^2, \\ \text{s.t.} \quad & \text{rank}(\mathcal{Y}) \leq r \end{aligned} \quad (5)$$

There are multiple ways to define the rank for tensors. For example, the definition based on Candecomp/Parafac (CP) decomposition [15]

$$\text{Rank}(\mathcal{Y}) = \min \left\{ r \mid \mathcal{Y} = \sum_{i=1}^r \mathbf{a}_i \circ \mathbf{b}_i \circ \mathbf{c}_i \right\}, \quad (6)$$



---

**Algorithm 2** Efficient Algorithm for Computing the Sparse Low-rank Approximation of the Matrix  $\mathbf{X}$ 


---

```

1: Input:  $\mathbf{X} \in \mathbb{R}^{N \times TC}$ , support set  $\Omega$ , rank  $r$ , number of iterations  $T$ 
2: Initialization: Gaussian random matrix  $\mathbf{R} \in \mathbb{R}^{TC \times r}$  satisfying  $\mathbf{R}_{ij} \sim \mathcal{N}(0, 1)$ ,  $\mathbf{Y} \leftarrow \mathbf{0}^{N \times TC}$ 
3:  $\mathbf{B} \leftarrow \mathbf{X}\mathbf{R}$ 
4:  $\mathbf{Q} \leftarrow QR(\mathbf{B})$ 
5: for  $t = 1, 2, \dots, m$  do
6:    $\mathbf{B} \leftarrow \mathbf{X}(\mathbf{X}^\top \mathbf{Q})$ 
7:    $\mathbf{Q} \leftarrow QR(\mathbf{B})$ 
8: end for
9:  $\mathbf{C} \leftarrow \mathbf{Q}^\top \mathbf{X}$ 
10:  $\mathbf{Y} \in \mathbb{R}^{N \times TC}$ :  $\mathbf{Y}_{ik} \leftarrow \mathbf{Q}_i \mathbf{C}_{:k}$ ,  $\exists j$ ,  $k \in \Omega_{ij}$ 
11: Output: sparse low-rank approximation  $\mathbf{Y}$ 

```

---

where  $\mathbf{a}_i \in \mathbb{R}^N$ ,  $\mathbf{b}_i \in \mathbb{R}^T$ ,  $\mathbf{c}_i \in \mathbb{R}^C$ , and the symbol  $\circ$  represents the vector outer product. Note that all CP rank involved problems are NP-hard in general [11]. Although many heuristic algorithms have been developed to increase the efficiency of CP decomposition [9, 20, 21, 14], they are still not scalable enough to handle our real-world location category inference problem that involves a large number of users and time slots. As a concrete example, recovering a rank 10 tensor of size  $500 \times 500 \times 500$  takes the state-of-the-art tensor factorization algorithm TenALS<sup>1</sup> more than 20,000 seconds on an Intel Xeon 2.40 GHz processor with 64 GB main memory.

In order to significantly improve the scalability of the proposed model in (5), we use the rank of the unfolding matrix as the rank of the tensor. Considering the correlation of users's behaviors is dominant in all correlation, we define the unfolding of our 3-order tensor  $\mathcal{Y} \in \mathbb{R}^{N \times T \times C}$  by merging the second (time) and third (location categories) indices of tensors as the column index of matrices. In other words,  $\mathbf{Y}$  is the concatenates of  $\mathcal{Y}$ 's lateral slices along the time mode, i.e.,

$$\mathbf{Y} = \text{Unfold}(\mathcal{Y}) := [\mathcal{Y}_{:1:} \cdots \mathcal{Y}_{:T:}] \in \mathbb{R}^{N \times TC}.$$

Then the tensor rank is defined as the matrix rank

$$\text{rank}(\mathcal{Y}) = \text{rank}(\text{Unfold}(\mathcal{Y})).$$

Therefore, our target problem can be cast into the following equivalent matrix optimization problem

$$\begin{aligned} \min_{\mathcal{Y} \in \mathbb{R}^{N \times T \times C}} \quad & \|\mathcal{X} - \mathcal{Y}\|_F^2 = \|\mathbf{X} - \mathbf{Y}\|_F^2, \\ \text{s.t.} \quad & \text{rank}(\text{Unfold}(\mathcal{Y})) \leq r, \end{aligned} \tag{7}$$

where  $\mathbf{X} = \text{Unfold}(\mathcal{X})$ . This problem can be solved efficiently via Algorithm 2.

Problem (7) essentially aims to find matrix  $\mathbf{X}$ 's best rank- $r$  approximation. Given  $\mathbf{X}$ 's singular value decomposition (SVD)  $\mathbf{U}\mathbf{\Sigma}\mathbf{V}^\top$ , it is well known that its best rank- $r$  approximation is given by  $\mathbf{U}_r \mathbf{\Sigma}_r \mathbf{V}_r^\top$ , where  $\mathbf{U}_r$ ,  $\mathbf{V}_r$  contain the first  $r$  columns of  $\mathbf{U}$  and  $\mathbf{V}$ , and  $\mathbf{\Sigma}_r$  is a diagonal matrix with the first  $r$  singular values lying on the diagonal. It can be done within a polynomial complexity, versus to the NP hardness of using the CP based definition for the tensor rank in (6). Although it is

---

<sup>1</sup><http://web.engr.illinois.edu/~swoh/software/optspace/code.html>

a big improvement from NP hard to polynomial time, it can be further improved since in practice we do not need computing SVD exactly. To this end, we efficiently compute its approximate SVD using the power method [10]. Besides, we notice that in the next step when  $\mathbf{Y}$  is fixed, only its entries inside the support  $\Omega$  are involved to update the matrix  $\mathbf{X}$ . In this sense, we do not need to compute  $\mathbf{Y}$ 's entries outside the support  $\Omega$  in the current step, thus allows us to further improve the efficiency. Algorithm 2 shows the detailed steps of the sparse low-rank approximation algorithm, where the notations  $\mathbf{Q}_{i:}$  and  $\mathbf{C}_{:k}$  represent the  $i$ -th row of  $\mathbf{Q}$  and the  $k$ -th row of  $\mathbf{C}$ , respectively.  $QR(\cdot)$  indicates the reduced QR factorization. In Algorithm 2, we assume that  $N \geq TC$ . Otherwise, we use  $\mathbf{X}^\top$  as its input thus the time complexity is dependent to  $\min(N, TC)$ .

### Total Complexity

Since  $\mathbf{X}$  is a sparse matrix with only  $|\Omega|$  non-zero entries, the computational cost of the steps 3, 6, 9, and 10 in Algorithm 2 are merely  $O(|\Omega|r)$ . In addition, since  $\mathbf{B} \in \mathbb{R}^{N \times r}$  is a tall-and-skinny matrix, its QR factorization can be efficiently computed using  $O(Nr^2)$  operations. Indeed, we can further reduce this cost if  $N > TC$ , in which case we use  $\mathbf{X}^\top$  instead of  $\mathbf{X}$  as Algorithm 2's input. In this way, the QR decomposition can be computed using  $O(TCr^2)$  operations. Combining all the computations together, we can update  $\mathbf{Y}$  within  $O(|\Omega|rm + \min(N, TC)r^2m)$  time, where  $m$  is the number of iterations. Since  $|\Omega| \ll NTC$  and  $r \ll \min(N, TC)$ , the proposed algorithm is significantly faster than the naive SVD computation with  $O(\max(N, TC) \min(N, TC)^2)$  complexity.

When the sparse low-rank approximation matrix  $\mathbf{Y}$  is learned, we update  $\mathbf{X}$  by projecting  $\mathbf{Y}$  to a space that satisfies the NU constraints (4). Although this step is efficient enough in the tensor case, it becomes even simpler in the matrix setting. Since  $\mathbf{Y}$  is already a sparse matrix with only  $|\Omega|$  non-zero entries, we only need to project each vector within  $\Omega_{ij}, \forall i, j$  onto the probability simplex. The time complexity of this step is  $O(\sum_{i,j} |\Omega_{ij}| \log(|\Omega_{ij}|))$ . Since we have  $|\Omega_{ij}| \leq C \forall i, j$ , this time complexity is upper bounded by  $O(|\Omega| \log C)$ .

Overall, each iteration (updating  $\mathbf{X}$  and  $\mathbf{Y}$  once) of the proposed alternating minimization algorithm can be efficiently computed within

$$O(|\Omega|(rm + \log C) + \min(N, TC)r^2m)$$

time. In addition to the low computational cost in each iteration, our algorithm converges very fast as well, as verified by extensive experiments on both simulated and real-world datasets. For example, it takes only 3 iterations to optimize a problem with 3 million users, 500 time slots, 200 location categories, and more than a billion non-zero entries in  $\Omega$ , with a running time for each single iteration about 18 minutes.

## 4 Experiments

In this section, we first conduct a simulated study to validate the scalability of the proposed algorithm – it is scalable to large-scale category inference problems. We then evaluate the proposed algorithm on multiple real-world mobility data sets. All experiments were run on a Linux server with an Intel Xeon 2.40 GHz CPU and 64 GB of main memory.

### 4.1 Synthesized Data Experiments

We first conduct experiments with simulated data to verify that the proposed location category inference algorithm is computationally efficient and robust to location errors. To this end, we fix  $T$  and

Table 1: CPU time and prediction accuracies with different number of users and location updates. K, M, B indicates thousands, millions, and billions, respectively.

#users	#time slots	#location categories	$ \Omega $	CPU Time (s)	Prediction Accuracy
100 K	500	200	40 M	124	100%
200 K	500	200	80 M	240	100%
500 K	500	200	200 M	660	100%
1 M	500	200	400 M	1,310	100%
2 M	500	200	800 M	1,938	100%
3 M	500	200	1.2 B	3,397	100%

$C$ , the number of time slots and the number of location categories, to 500 and 200, respectively. We also vary the number of mobile phone users,  $N$ , in range  $\{100 \text{ K}, 200 \text{ K}, 500 \text{ K}, 1 \text{ M}, 2 \text{ M}, 3 \text{ M}\}$ , where K and M stand for thousand(s) and million(s), respectively. For a fixed  $N$ , we randomly assign all the mobile phone users to 10 lifestyle classes, with the class memberships blind to our algorithm. We assume that users in the same lifestyle class visit the same location categories at the same time while users in different classes behave differently. For each user and 20% of the randomly sampled time slots, we generate her noisy location updates that contain 4 candidate location categories for each of them. Among the 4 candidate categories, one is the true location category and the other three are randomly sampled from the remained  $C - 1$  location categories. We input the generated location updates data to our algorithm and compare the predicted results with the ground truth information. Table 1 summarizes the CPU time and prediction accuracies of inferring location categories on this data. Specifically, the prediction accuracy is defined as

$$\frac{\text{\#(category with the highest prob. = true category)}}{\text{\#location updates}} \times 100\%.$$

Table 1 clearly shows that the proposed algorithm can *perfectly* recover the underlying true location categories as all the prediction accuracies equal to 100%. Besides, the proposed algorithm is extremely efficient, e.g., even with 3 million users and more than 1 billion candidate location categories, it only takes the proposed algorithm less than 2 hours to infer the perfect location category in a single thread.

## 4.2 Real-World Location Update Data Experiments

### Data Preprocessing

The real-world location update data consists of a temporal stream of records in the form  $\{\textit{anonymous user id}, \textit{UTC timestamp}, \textit{estimated location coordinates}, \textit{location error}\}$ , in order to apply our location category inference algorithm, the raw data was preprocessed, encompassing three key steps: 1) removal of noise to obtain meaningful location coordinates, 2) association of meaningful locations with candidate venues (and hence categories), and 3) determination of the local time and quantization into time slots.

The first step is necessary because we are only interested in locations where the user has spent significant time – locations that could have actually been visited in a meaningful way. In addition, the dynamics of mobile phone location update algorithms may not be completely understood. For

example, the significant-change location service, a frequently used location API on iOS devices, “delivers updates only when there has been a significant change in the device’s location, such as 500 meters or more.”<sup>2</sup> Also, under this set of location APIs, the precise triggers which initiate an update are not fully disclosed. To determine meaningful locations, the first step is to estimate the dwell time by taking the difference of subsequent timestamps. Once dwell time is estimated, locations where the dwell time is less than a threshold are removed.

The next step in the process is to associate the location update coordinates to venues. In our case, Foursquare APIs<sup>3</sup> were used to query for potential venues. Specifically, we define the location uncertainty circle for an update as the circle centered on the update coordinates with radius given by the reported location error,  $r_{\text{error}}$ . Similarly, we represent a venue as a circle with a fixed radius  $r_{\text{venue}}$  centered on the venue coordinates. Then, a venue is considered a candidate venue if it intersects with the location uncertainty circle, i.e., if  $h(\mathbf{x}, \mathbf{p}) \leq r_{\text{error}} + r_{\text{venue}}$ . Here,  $h(\cdot, \cdot)$  is the haversine distance between the location update  $\mathbf{x}$  and the venue coordinates  $\mathbf{p}$ . Once a candidate set of venues is known for a location update, the category information is extracted. We used a subset of 42 of the available categories from the Foursquare hierarchy. The categories were chosen to cover the entire hierarchy, and any categories falling below a chosen category were mapped to its closest ancestor category. Categories chosen include: Museum, College & University, Music Venue, Train Station, etc.

Finally, we convert all timestamps into local time to better understand the context of a user’s visit. This is done by determining the local timezone based on the coordinates and then adjusting the UTC timestamp using the appropriate offset. Finally the timestamps are quantized, non-uniformly, into time slots across each day using the following process. The time period from 1am to 7am is mapped to the first bin, 7am-9am is mapped to the second bin, 9am-11am is mapped to the third bin, etc., giving 10 bins per day. The non-uniform scheme is chosen since there is little activity during the early morning.

## Experiments

We ran experiments across three major U.S. cities, New York city, NY, Austin, TX, and San Francisco, CA, using anonymized mobile location data that was collected as part of an IBM partnership with a leading location-based services company. The cities were defined by considering the bounding box that contains the metropolitan statistical area, as defined by the U.S. government. For each city we looked at 2 weeks of location update data. We considered location updates which corresponded to a dwell time of at least 20 minutes. Finally we considered users who had updates on at least 7 days, with a total of at least 50 updates. The statistics of the three datasets are shown in Table 2.

In order to evaluate the performance, we look for location updates where there is no category ambiguity, i.e., there was only one location category within the user’s location uncertainty circle. These true location categories are used as the validation set. For the same user-timeslot pairs in the validation set we also create noisy data by marking all the  $C$  location categories as the possible categories. This noisy data set is combined with original data, less the validation set, and used as the input to our algorithm. After learning the tensor  $\mathcal{X}$ , we check, for each location update in the validation set, if the categories with the top  $k$  highest probabilities contain the true venue category.

<sup>2</sup><https://developer.apple.com/library/content/documentation/UserExperience/Conceptual/LocationAwarenessPG/CoreLocation/CoreLocation.html>

<sup>3</sup><https://developer.foursquare.com/docs/>

Table 2: Statistics of the three location updates data sets

Data sets	# users	# time slots	# location categories
New York, NY	77,084	138	42
Austin, TX	10,211	137	42
San Francisco, CA	11,083	138	42

We set  $k = \{1, 2, \dots, 5\}$  in our study. In particular,  $k = 1$  means that the true venue category is consistent with the learned highest probability category.

Since our proposed NUTF is, to the best of our knowledge, the first algorithm that can infer location categories based on inaccurate mobility location data, there is no direct baseline for comparison. Note that our validation set contains the location updates with only one location category within their corresponding location uncertainty circles. We cannot compare our method with 1-NN approach since its results are trivial, i.e., the only one location category in a location uncertainty circle is always the nearest neighbor. In this case, we compare our negative-unlabeled tensor factorization approach with three state-of-the-art tensor factorization algorithms: (a) **CP-APR**, Candecomp-Parafac alternating Poisson regression [7], (b) **Rubik**, knowledge-guided tensor factorization and completion method [24], and (c) **BPTF**, Bayesian probabilistic tensor factorization [27]. To this end, given a set of  $N$  users,  $T$  time slots, and  $C$  location categories, we generate a  $N \times T \times C$  partially-observed tensor  $\mathcal{W}$  as

$$\mathcal{W}_{ijk} = \begin{cases} 0.1, & \text{if } k \in \Omega_{ij}, \text{ and with a probability } p \\ \text{unobserved}, & \text{if } k \in \Omega_{ij}, \text{ and with a probability } 1 - p \\ 0, & \text{if } k \notin \Omega_{ij}, \end{cases}$$

where the probability  $p$  is set to be 20% in our study. We use this tensor to simulate our condition where all the location categories not covered by the location uncertainty circle are impossible ( $=0$ ), and the location categories covered by the circle have unknown probabilities with some samples having the same initialization ( $=0.1$ ). We then use the tensor  $\mathcal{W}$ , with all the entries in the validation set marked as unobserved, as an input to our baseline tensor factorization algorithms to recover its low-rank approximations. Given the tensor recovered by the baseline algorithms, we check, for each location update in the validation set, if the categories with the top  $k$  highest probabilities contain the true venue category — identical to the way used to evaluate our method.

Table 3 summarizes the prediction performance averaged over the five trials of all the algorithms. We first observe that the prediction accuracies of the proposed method NUTF are very encouraging. Among all the three data sets, its exact matching ( $k=1$ ) accuracies range from 32% to 35%, and its top 5 category accuracies range from 75% to 79%. Given that these data sets have a total of 42 location categories and a random guess only yields a 2.4% accuracy, our prediction performance clearly demonstrates the effectiveness of the proposed method. In addition, our method NUTF also yields significantly better performance than all the baseline algorithms. In particular, its accuracies are about 3 times better than the baselines. Finally, we observe that the prediction performance of all the algorithms is fairly consistent across the three cities, suggesting that our collected data is sufficiently representative.

Table 3: Prediction accuracies of the proposed algorithm NUTF and three baseline algorithms on the three real-world location updates data. N/A indicates that the factorization task could not be completed due to memory limitations.

Data sets	k	NUTF	CP-APR	Rubik	BPTF
New York, NY	1	<b>35%</b>	N/A	12%	10%
	2	<b>54%</b>	N/A	15%	14%
	3	<b>67%</b>	N/A	19%	17%
	4	<b>74%</b>	N/A	21%	19%
	5	<b>79%</b>	N/A	24%	21%
Austin, TX	1	<b>34%</b>	11%	12%	9%
	2	<b>52%</b>	13%	14%	11%
	3	<b>65%</b>	16%	18%	16%
	4	<b>73%</b>	20%	21%	19%
	5	<b>78%</b>	23%	23%	22%
San Francisco, CA	1	<b>32%</b>	11%	11%	9%
	2	<b>50%</b>	12%	14%	11%
	3	<b>63%</b>	15%	17%	17%
	4	<b>70%</b>	20%	21%	19%
	5	<b>75%</b>	22%	23%	21%

### 4.3 Real-World Check-in Data Experiments

In addition to the experiments with the mobility location updates data, we conduct experiments on two real-world check-in data sets to verify that the proposed algorithm can also reliably infer users' location categories even when there is no location update. The two data sets collected by [28] consist of the Foursquare check-ins in New York City (NYC) and Tokyo from 12 April 2012 to 16 February 2013. The New York check-in data set contains 824 users, 38,336 venues and 227,428 check-ins, while the Tokyo check-in data contains 1,939 users, 61,858 venues, and 573,703 check-in records. Each check-in includes a user ID, a time stamp, a venue ID, and the category of the venue. By manually merging the similar and infrequent venue categories together, we finally obtain 122 venue categories for both data sets. Similar to the experiments with the mobility location updates data, we use hourly time slot and select the check-in with the longest dwell time if there are more than one check-ins within a same time slot.

In order to evaluate our performance, we randomly sample 10% of the check-ins as the validation set, and mark all the  $C$  location categories as the possible categories for all of them. This mimics the situation when there is no available location update, or the location update is too inaccurate to contain any meaningful location information. We then combine the noisy and accurate check-ins altogether and use them as the input to our algorithm. After learning the tensor  $\mathcal{X}$ , we check that, for each check-in in the validation set, if the categories with the top  $k$  highest probabilities contain the true venue category. We set  $k = \{1, 2, \dots, 5\}$  in our study. In particular,  $k = 1$

Table 4: Average prediction accuracies of the proposed algorithm NUTF, and the baseline algorithms PU-MC and WR-MF when  $k = 1, 2, \dots, 5$ .

Data sets	k	NUTF	PU-MC	WR-MF
NYC Check-ins	1	<b>30%</b>	8%	19%
	2	<b>43%</b>	14%	30%
	3	<b>50%</b>	18%	37%
	4	<b>55%</b>	21%	42%
	5	<b>58%</b>	25%	46%
Tokyo Check-ins	1	<b>46%</b>	12%	40%
	2	<b>60%</b>	19%	53%
	3	<b>67%</b>	23%	62%
	4	<b>71%</b>	27%	67%
	5	<b>74%</b>	29%	71%

Table 5: Average CPU time (in seconds) of the proposed algorithm NUTF, and the baseline algorithms PU-MC and WR-MF

Data sets	NUTF	PU-MC	WR-MF
NYC Check-ins	<b>4.8</b>	599	14
Tokyo Check-ins	<b>12</b>	498	48

means that the true venue category is consistent with the learned highest probability category.

To find baseline algorithms for this study, we cast this problem into a matrix completion problem [5]. Let  $N$ ,  $T$ , and  $C$  be the number of users, time slots, and location categories, respectively. Given the training check-in records that do not belong to the validation set, we construct a  $N \times TC$  partially-observed matrix with the observed entries corresponding to the check-ins. In this sense, the prediction problem becomes a matrix completion problem that aims to recover the unobserved entries based on the observed ones. Also, since all the observed entries are drawn from the positive (interest) class, this is a positive-unlabeled (PU) learning problem. We thus compare our method with the state-of-the-art PU matrix completion algorithms: (a) **PU-MC**, PU learning for matrix completion [12], and (b) **WR-MF**, weighted regularized matrix factorization [13]. Specifically, we feed the generated partially-observed matrix to these algorithms, and compare the ground-truth venue categories in the validation set with their corresponding outputs. All the experiments in this study are repeated five times, and the prediction accuracies and the running time averaged over the five trials are reported in Table 4 and Table 5, respectively.

Table 4 summarizes the average prediction accuracies of the proposed algorithm NUTF, and the baseline algorithms PU-MC and WR-MF when  $k = 1, 2, \dots, 5$ . It clearly shows that the proposed algorithm NUTF significantly outperforms all the baseline algorithms. Specifically, 30% and 46% of the learned highest probability categories are consistent with the ground truth categories

of the NYC check-ins and Tokyo check-ins data sets, respectively. Considering that we have 122 categories in total, the achieved accuracies are pretty impressive. In addition, Table 5 summarizes the average CPU time of the all the algorithms evaluated here. Among them, our proposed method NUTF is the most efficient algorithm. In particular, NUTF is able to infer the location categories of the Tokyo Check-ins data in 12 seconds.

Another interesting finding in this study is that all the algorithms perform better on the Tokyo data than on the NYC data. This is because the Tokyo data set is larger with more users and more check-in records. Since all the algorithms evaluated here are collaborative approaches that learn a universal model from all the available user data, they usually deliver more accurate results as more data is provided.

## 5 Conclusions

In this paper, we study the problem of inferring the user visited location categories purely based on their inaccurate mobility location data. To the best of our knowledge, our paper is the first study of this kind. To solve this problem, we propose a novel tensor factorization framework NUTF that is able to infer the most likely location categories within the location uncertainty circle. To this end, we highlight several key observations, including the negative-unlabeled constraints and the correlations among users. In order to efficiently solve the tensor factorization problem, we propose a parameter-free and scalable optimization algorithm by effectively exploring the sparse and low-rank structure of the underlying tensor. Our empirical studies conducted on multiple synthesized and real-world data sets confirm both the effectiveness and efficiency of the proposed algorithm.

## References

- [1] Daniel Ashbrook and Thad Starner. Using gps to learn significant locations and predict movement across multiple users. *Personal and Ubiquitous computing*, 7(5):275–286, 2003.
- [2] Linas Baltrunas and Xavier Amatriain. Towards time-dependant recommendation based on implicit feedback. In *Workshop on context-aware recommender systems*, 2009.
- [3] Jie Bao, Yu Zheng, David Wilkie, and Mohamed Mokbel. Recommendations in location-based social networks: a survey. *GeoInformatica*, 19(3):525–565, 2015.
- [4] Sean J Barbeau, Philip L Winters, Nevine L Georggi, Miguel A Labrador, and Rafael Perez. Travel assistance device: utilising global positioning system-enabled mobile phones to aid transit riders with special needs. *IET intelligent transport systems*, 4(1):12–23, 2010.
- [5] Emmanuel Candes and Benjamin Recht. Exact matrix completion via convex optimization. *Communications of the ACM*, 55(6):111–119, 2012.
- [6] Xin Cao, Gao Cong, and Christian S Jensen. Mining significant semantic locations from gps data. *Proceedings of the VLDB Endowment*, 3(1-2):1009–1020, 2010.
- [7] Eric C. Chi and Tamara G. Kolda. On tensors, sparsity, and nonnegative factorizations. *SIAM Journal on Matrix Analysis and Applications*, 33(4):1272–1299, 2012.



- [8] Charles Elkan and Keith Noto. Learning classifiers from only positive and unlabeled data. In *KDD*, pages 213–220, 2008.
- [9] Mike Espig and Wolfgang Hackbusch. A regularized newton method for the efficient approximation of tensors represented in the canonical tensor format. *Numerische Mathematik*, 122(3):489–525, 2012.
- [10] Nathan Halko, Per-Gunnar Martinsson, and Joel A Tropp. Finding structure with randomness: Probabilistic algorithms for constructing approximate matrix decompositions. *SIAM review*, 53(2):217–288, 2011.
- [11] Christopher J Hillar and Lek-Heng Lim. Most tensor problems are np-hard. *Journal of the ACM (JACM)*, 60(6):45, 2013.
- [12] Cho-Jui Hsieh, Nagarajan Natarajan, and Inderjit S. Dhillon. PU learning for matrix completion. In *ICML*, pages 2445–2453, 2015.
- [13] Yifan Hu, Yehuda Koren, and Chris Volinsky. Collaborative filtering for implicit feedback datasets. In *Data Mining, 2008. ICDM’08. Eighth IEEE International Conference on*, pages 263–272. Ieee, 2008.
- [14] Prateek Jain and Sewoong Oh. Provable tensor factorization with missing data. In *NIPS*, pages 1431–1439, 2014.
- [15] Tamara G Kolda and Brett W Bader. Tensor decompositions and applications. *SIAM review*, 51(3):455–500, 2009.
- [16] Quannan Li, Yu Zheng, Xing Xie, Yukun Chen, Wenyu Liu, and Wei-Ying Ma. Mining user similarity based on location history. In *Proceedings of the 16th ACM SIGSPATIAL international conference on Advances in geographic information systems*, page 34. ACM, 2008.
- [17] Bing Liu, Yang Dai, Xiaoli Li, Wee Sun Lee, and Philip S. Yu. Building text classifiers using positive and unlabeled examples. In *ICML*, pages 179–188, 2003.
- [18] Rong Liu, Swapna Buccapatnam, Wesley M Gifford, and Anshul Sheopuri. An unsupervised collaborative approach to identifying home and work locations. In *Mobile Data Management (MDM), 2016 17th IEEE International Conference on*, volume 1, pages 310–317. IEEE, 2016.
- [19] Prashanth Mohan, Venkata N Padmanabhan, and Ramachandran Ramjee. Nericell: rich monitoring of road and traffic conditions using mobile smartphones. In *Proceedings of the 6th ACM conference on Embedded network sensor systems*, pages 323–336. ACM, 2008.
- [20] Anh-Huy Phan, Petr Tichavsky, and Andrzej Cichocki. Low complexity damped gauss–newton algorithms for candecomp/parafac. *SIAM Journal on Matrix Analysis and Applications*, 34(1):126–147, 2013.
- [21] Myriam Rajih, Pierre Comon, and Richard A Harshman. Enhanced line search: A novel method to accelerate parafac. *SIAM journal on matrix analysis and applications*, 30(3):1128–1147, 2008.

- [22] Steffen Rendle, Christoph Freudenthaler, Zeno Gantner, and Lars Schmidt-Thieme. BPR: bayesian personalized ranking from implicit feedback. In *UAI*, pages 452–461, 2009.
- [23] Weiran Wang and Miguel Á. Carreira-Perpiñán. Projection onto the probability simplex: An efficient algorithm with a simple proof, and an application. *CoRR*, abs/1309.1541, 2013.
- [24] Yichen Wang, Robert Chen, Joydeep Ghosh, Joshua C. Denny, Abel N. Kho, You Chen, Bradley A. Malin, and Jimeng Sun. Rubik: Knowledge guided tensor factorization and completion for health data analytics. In *SIGKDD*, pages 1265–1274, 2015.
- [25] Yilun Wang, Yu Zheng, and Yexiang Xue. Travel time estimation of a path using sparse trajectories. In *SIGKDD*, pages 25–34, 2014.
- [26] Xiangye Xiao, Yu Zheng, Qiong Luo, and Xing Xie. Finding similar users using category-based location history. In *Proceedings of the 18th SIGSPATIAL International Conference on Advances in Geographic Information Systems*, pages 442–445. ACM, 2010.
- [27] Liang Xiong, Xi Chen, Tzu-Kuo Huang, Jeff G. Schneider, and Jaime G. Carbonell. Temporal collaborative filtering with bayesian probabilistic tensor factorization. In *SDM*, pages 211–222, 2010.
- [28] Dingqi Yang, Daqing Zhang, Vincent W Zheng, and Zhiyong Yu. Modeling user activity preference by leveraging user spatial temporal characteristics in lbsns. *IEEE Transactions on Systems, Man, and Cybernetics: Systems*, 45(1):129–142, 2015.
- [29] Yang Ye, Yu Zheng, Yukun Chen, Jianhua Feng, and Xing Xie. Mining individual life pattern based on location history. In *Mobile Data Management: Systems, Services and Middleware, 2009. MDM’09. Tenth International Conference on*, pages 1–10. IEEE, 2009.
- [30] Jing Yuan, Yu Zheng, Liuhang Zhang, Xing Xie, and Guangzhong Sun. Where to find my next passenger. In *Proceedings of the 13th international conference on Ubiquitous computing*, pages 109–118. ACM, 2011.
- [31] Nicholas Jing Yuan, Yu Zheng, Liuhang Zhang, and Xing Xie. T-finder: A recommender system for finding passengers and vacant taxis. *IEEE Transactions on Knowledge and Data Engineering*, 25(10):2390–2403, 2013.
- [32] Yu Zheng. Trajectory data mining: an overview. *ACM Transactions on Intelligent Systems and Technology (TIST)*, 6(3):29, 2015.
- [33] Yu Zheng, Licia Capra, Ouri Wolfson, and Hai Yang. Urban computing: concepts, methodologies, and applications. *ACM Transactions on Intelligent Systems and Technology (TIST)*, 5(3):38, 2014.
- [34] Changqing Zhou, Nupur Bhatnagar, Shashi Shekhar, and Loren Terveen. Mining personally important places from gps tracks. In *Data Engineering Workshop, 2007 IEEE 23rd International Conference on*, pages 517–526. IEEE, 2007.